Miniaturized Samples for Bond Strength and Hermetic Sealing Evaluation for Transmission Laser Joints

Golam Newaz[1, 2], Taslema Sultana[2, 3], Saied Nusier[1] and Hans J. Herfurth[4]

[1]*Department of Mechanical Engineering, 5050 Anthony Wayne Dr., Detroit, MI 48202, USA*
[2]*Institute for Manufacturing Research, Wayne State University, 666 Hancock Ave., Detroit, MI 48202*
E-mail: gnewaz@eng.wayne.edu
[3]*Department of Chemical Engineering and Materials Science, 5050 Anthony Wayne Dr., Detroit, MI 48202, USA*
[4]*Fraunhofer Center for Laser Technology, 46025 Port St., Plymouth, MI 48170, USA*

Transmission laser bonded titanium coated glass/polyimide miniature samples were tested to find out bond strength and hermeticity. Bond strength was evaluated using a miniature lap shear specimen and by developing a pressure test specimen. The joint hermeticity was tested by Helium bomb test. Successful results from these tests and meaningful failure modes establish these tests as good methods to determine the integrity of the joints. This paper will analyze the results and provide the technical basis for utilizing these tests for reliable assessment of the quality of transmission laser joints.

DOI: 10.2961/jlmn.2008.03.0011

Keywords: miniaturized sample, transmission laser joint, bond strength, hermeticity, near-hermetic packaging

1. Introduction

Micro-joining of organic materials to different materials like metal, glass or silicon could play an important role in optoelectronic and biomedical applications [1, 2]. Organic materials have a "near-hermetic" categorization and could be adequate to provide acceptable microelectronics packaging characteristics for intermediate to long lifetimes at a fraction of the price, weight, and size of current hermetic packaging solutions [3]. The use of a sufficient quantity of an efficient moisture getter should allow near-hermetic packages to be used for microelectronic systems [4]. To bond plastics to other materials, it is necessary that the system does not alter the properties and performance of plastic materials. Also, the system should provide high integration, hermetic sealing and automated assembly. Yu-Chuan Su et al. used micro-heater to bond plastic to other materials [5]. Ultrasonic welding may also be used. We used transmission laser joining technique to join a thermoplastic polyimide Imidex to Pyrex 7740 borosilicate glass. The process has been explained in detail in references [6-12]. Low power (<30 W) fiber laser beam having Gaussian power profile is used to develop the bonding processes. The key features of the laser joining technique include localized joint with minimal heat affected zone (HAZ), flexibility, shorter processing time and higher quality. Suitable laser parameter ranges for joining the Ti coated glass/Imidex combination are determined by Fraunhofer Center for Laser Technology (CLT), USA.

Glass has higher planarity and lower cost than the ceramics and has drawn an attention as the packaging substrate material. A glass substrate is excellent in high frequency characteristics and is expected to be mounted to mobile communication devices [3]. Pyrex is made to withstand thermal shock better than most other glass through a combination of reduced expansion coefficient and greater strength [13]. For transmission laser joining, a thin layer of metal coating is applied on glass to act as coupling agent. Titanium is selected as the coating material because it provides certain levels of biocompatibility for specific applications [14]. Thermoplastic polyimide Imidex is chosen as one of the joining material because thermoplastics have long molecular chains that are independent and not linked, so when sufficient heat is applied, the chains can move and the plastic can flow and be shaped. Upon cooling, the material is returned to the solid state with no significant material change. This glass/polyimide combination is a very promising system in life science such as neural stimulator devices or implantable sensors in human body, microfluidic devices and also in optoelectronic devices such as device packaging.

This paper describes in detail the miniature lap shear testing, pressure testing and hermeticity testing procedures to evaluate the Ti coated glass/Imidex laser joint strength and hermeticity. Chemical analysis in the lap shear joint region was performed by using X-ray Photoelectron Spectroscopy (XPS). Failure mode analysis of lap shear and pressure tested samples was done using optical microscopy and Scanning Electron Microscopy (SEM). Commercially available Finite Element Analysis (FEA) package ABAQUS [15] was used to develop finite element models to better understand the stress distribution within the joining area of the lap shear samples while the system was loaded with tension. Dynamic model was developed using shell elements to predict pressure test sample joint strength. LS-DYNA code was used in the modeling.

2. Sample preparation

Pyrex 7740 borosilicate glass wafers of 0.5 mm thickness (Corning) were coated with titanium (Ti) film (~0.2 μm thickness) by cathodic arc Physical Vapor Deposition (PVD) method. These Ti-coated glass wafers were joined with polyimide (Imidex [16]) films (0.18 mm thick) from Westlake Plastics Company. One set of samples were prepared for doing mechanical lap shear test. The lap shear test sample geometry is shown in Fig. 1. The other set of samples (pressure test samples) have dimension of W 3.0 mm x L 5.0 mm x T 0.68 mm. Imidex film of approximately 2 mm diameter is laser joined with Ti coated glass having dimension of W 3.0 mm x L 5.0 mm x T 0.5 mm. Fig. 2 shows the size of the samples compared to a US penny. The sample configuration and dimensions are shown in Fig. 3. Pressure testing samples have through hole so that high pressure can be used to break the laser joint. The hermeticity testing samples were specially designed with cavity in the glass wafer. The schematic diagram of the hermeticity test sample is shown in Fig. 4. The hermeticity test samples have internal volume of about 1.5×10^{-4} cm^3.

The laser joining procedure utilizes a beam of a continuous wave (cw) Yb-doped fiber laser (λ = 1100 nm). Transmission joining configuration was employed in which the laser energy penetrates the transparent part and is absorbed by the absorbing part, so that the heat is induced directly at the interface. The titanium on borosilicate glass works as a laser energy absorber. A clamping pressure of 210 kPa was applied. Two Borofloat glass blocks (thickness 11 mm) are used to hold the sample. The materials were ultrasonically cleaned with acetone and iso-propanol before joining. Imidex lay with the rough side toward the beam. The beam passed through one borofloat glass plate, then through the Imidex film and was then focused onto the Ti coated glass wafer which lies on another Borofloat glass block.

To prepare the lap shear test samples a clamping pressure of 415 kPa was used and laser beam with a total power of 1.0 W was used at a speed of 100 mm/min to generate 6.5-mm long joint. The overall bond width was observed to be 0.33 mm. Samples of this type with densely arranged parallel joint lines were also prepared for XPS measurements. To prepare the pressure test and hermeticity test samples, the laser beam with a total power of 1.01 W was used. A scanning speed of 100 mm/min was used for the first rotation and 150 mm/min for the second rotation to produce the 1.6 mm diameter joint lines. The joint width was 0.24 mm. It is mentioned here that defocusing of the beam is necessary to avoid overheating, degeneration and burning of the polyimide by lowering the intensity in the center of the laser spot. No observable damage, such as the interface detachment or any burning mark was found in the samples.

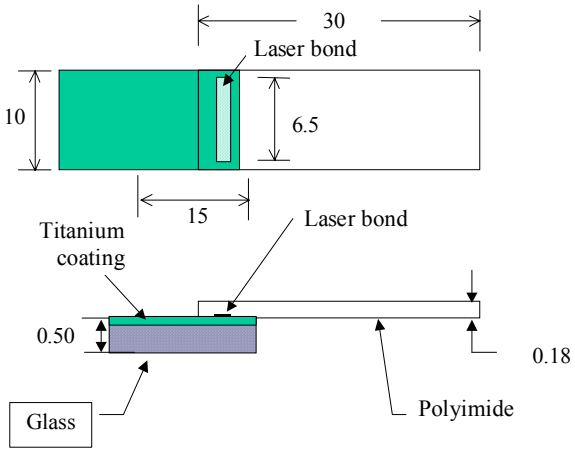

Fig. 1 Schematic diagram of lap shear test sample (All dimensions in mm – not in scale).

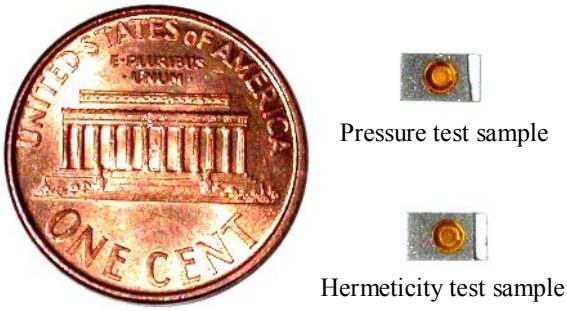

Fig. 2 The size of the pressure test and hermeticity test samples compared to a penny.

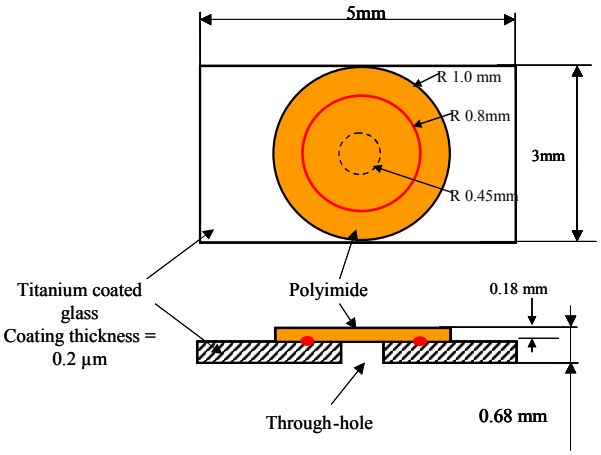

Fig. 3 Schematic of pressure testing sample

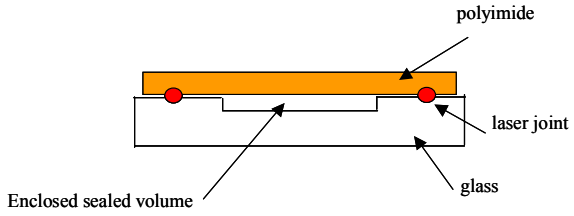

Fig. 4 Schematic of hermeticity testing samples.

3. Experiments

3.1 Lap shear test

A 6-axis microtester was used for doing lap shear test. The microtester is shown in Fig. 5. It is a general purpose micromechanical/thermal testing instrument, fully controlled by a computer [17]. Upon testing, samples were subjected to lap shear load by turning on a motor that moves a stage in the z-direction. A sample in the fixture is shown in Fig. 6. The samples were tested at a stage speed of 0.05 mm/s. The maximum load was set to 10 kg and maximum displacement to 50 mm. The software collects the load-displacement data. The failure loads obtained for all samples were normalized by the joint area as measured by the optical microscopy.

3.2 Pressure test

A schematic of the pressure testing set up is depicted in Fig. 7. High-pressure (10 MPa) nitrogen gas flows through the hole in the glass substrate and applies load directly on the polyimide film. A pressure sensor (Entran; Model: EPO-W31-175B) monitors the incremental pressure rise and the data is recorded as a function of load application time using a computer controlled Lab View based data acquisition software. The drop in applied pressure indicates the location of joint failure. The fixture was designed so that it can ensure hermetic sealing of the brittle glass/polyimide sample. Any gas leakage will cause reduction in gas pressure and the experiment will be interrupted. A sample hermetically sealed in the fixture is shown in Fig. 8. First, the sample is placed in the groove of the fixture above the O-ring. Another gasket is placed on the top of the sample around the polyimide film. A bolt is then tightened from the top to push down the sample. Precise care has to be taken while tightening the bolt. Glass being brittle, a smaller excessive turn can result in sample breakage. A sample in fixture is shown in Fig. 9.

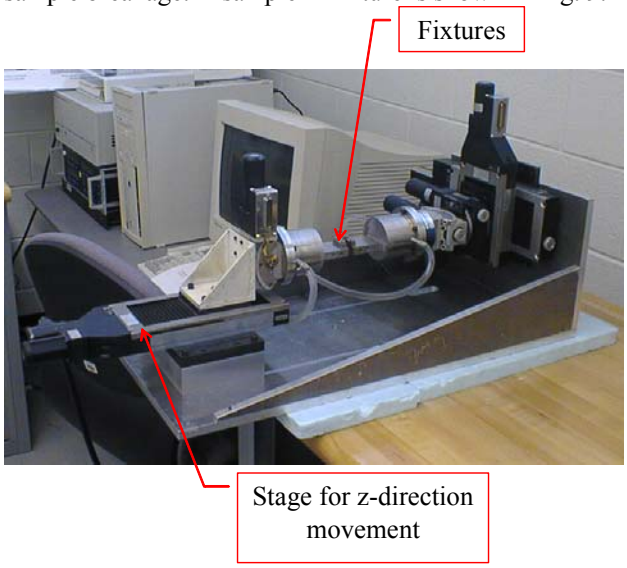

Fig. 5 Microtester for lap shear testing of the laser joint.

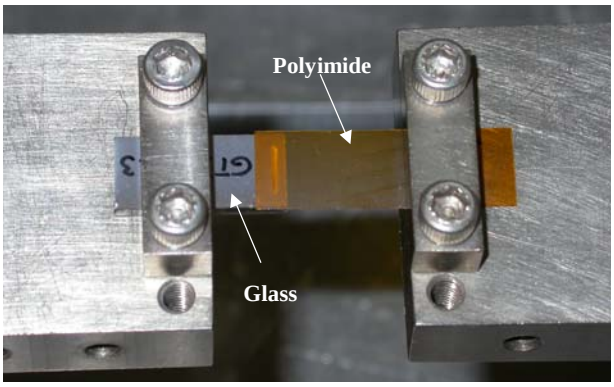

Fig. 6 A lap shear test sample in the microtester.

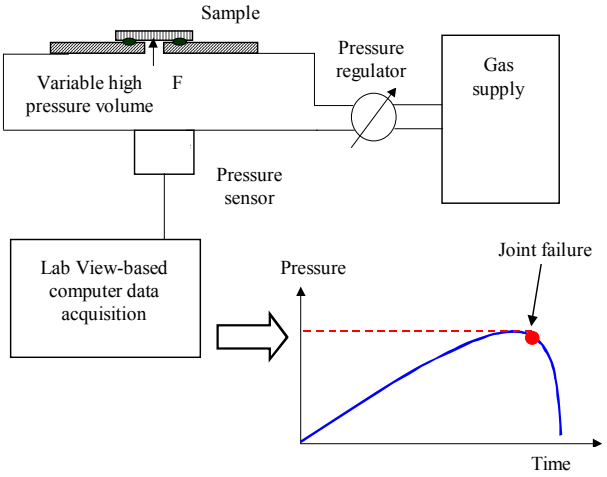

Fig. 7 A schematic of the pressure testing set up.

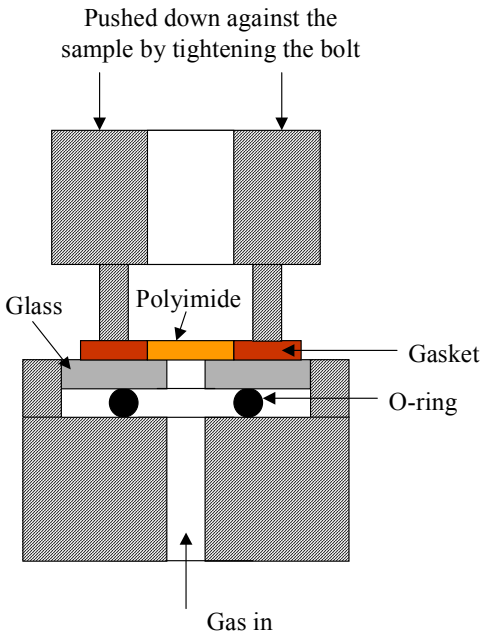

Fig. 8 A schematic diagram showing the method of sealing the sample in the test fixture.

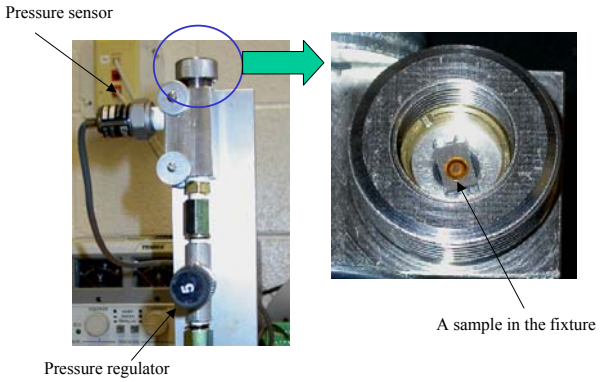

Fig. 9 A sample in the pressure test fixture

3.3 Helium bomb test

The hermeticity of the laser joints was measured by a Varian Contra-Flow He-leak tester, equipped with a turbo-molecular vacuum pump. This tester is capable of detecting leaks as small as 1×10^{-9} std. cc/sec and the measurements are done at a vacuum of 10mTorr after initial calibration with a He-leak calibration standard. Sealed samples are first placed in a high-pressure (345 kPa) chamber filled with He gas for a certain time (1 hour). After the "bombing" procedure (typically less than a minute after the samples are removed from the high-pressure chamber) the samples are placed in the vacuum test chamber of the He-leak tester and a leak rate is measured.

3.4 XPS analysis

The XPS samples were separated into their PI and Ti coated glass parts by peeling in air and immediately introduced in the UHV-analysis chamber of a Perkin Elmer model 5500 XPS spectrometer. Both sides of the joint were studied. A relatively large analysis area was used that averaged over several joint lines and inter-joint regions following the procedure outlined in [11]. This approach was found to provide a good signal-to-noise ratio, and it insured that the signal was originating from a known area of the peeled joint. Thus all spectra that were obtained contained a ~50% contribution from the non-laser-treated surface of the sample, and the spectral analysis needed to take this into account. The base vacuum pressure was 5×10−10 Torr and an Ar ion beam was used to sputter the sample surfaces in order to obtain spectra from various depths below the surface. A low-energy electron beam (neutralizer) was used to compensate for charging effects when studying the PI sheet (not needed in studying the Ti-coated glass plate).

3.5 SEM imaging

SEM images of the tested samples were taken in a Hitachi electron microscope, model S-2400. To avoid charging effects, the samples were sputter-coated (Ernest F. Fullam sputter coater) with a thin gold (Au) layer (20 s sputtering) prior to the SEM imaging.

3.7 Finite Element Analysis (FEA)

Since the Ti coating is very thin (thickness of 2 μm) compared to the glass and Imidex thicknesses, and since the stress distribution within all three mating materials near the bond is crucial for analysis purposes, a very refined mesh density is adopted near the bond using three noded CPE3 and four nodded CPE4 elements. The number of elements for glass, Imidex, and Ti portions were 26878, 7028, and 2591, respectively. The applied boundary and loading conditions, and mesh density near the bond are shown in Figure 10. Geometry of the model in Figure 10 represents true dimensions of the sample that was used for experiments that is given in Figure 4. The point where the edge of polyimide is bonded with titanium is designated as A, and the point where the edge of titanium is bonded to polyimide is designated as B (Fig. 10). Thus, the bond line between titanium and polyimide in this case is AB. In the model, the Ti-glass interface, and bond line AB between titanium and polyimide were considered to be strong. These strong bimaterial interfaces were modeled by using a common set of nodes at the glass-titanium and titanium-polyimide interfaces. Effect of thickness of the very thin chemical bond created between titanium and polyimide was neglected. The applied boundary conditions were such that glass end of the joint was clamped, i.e. no movements were allowed in either the horizontal (x) or vertical (y) direction. The other (polyimide) end was neglected. The applied boundary conditions were such that glass end of the joint was clamped, i.e. no movements were allowed in either the horizontal (x) or vertical (y) direction. The other (polyimide) end was restrained in the horizontal (x) direction, whereas its vertical (y-direction) nodal deflections were prescribed to be equal.

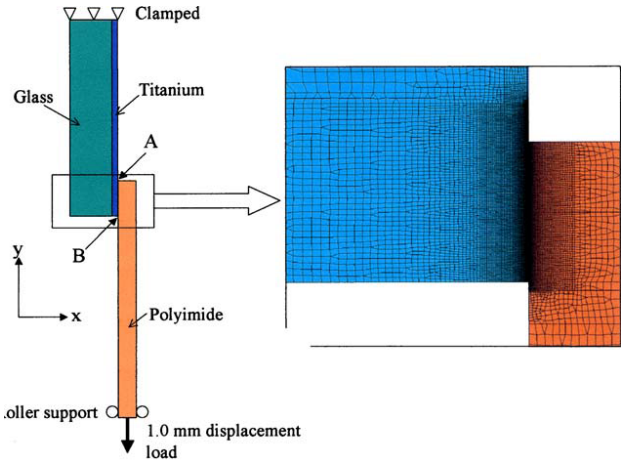

Fig. 10 Boundary Conditions and Zoomed-In Mesh view (FEA model).

A displacement of 0.12 mm was applied at the polyimide end with 20 incremental steps, and static analysis was performed. Load at every incremental step was calculated by summing up the reaction forces at the

fixed end. The reaction force per unit bond length was plotted against the incremental displacement load, and was compared with the experimental load displacement curves. Two material models such as a simple linear elastic model for glass and titanium, and linear elastic—plastic for polyimide were used in the study. The details of the model is discussed in reference [18].

4. Results and discussion

The average failure load of the lap shear test samples is 22.1 ± 1.3 MPa for the 6 samples tested. The pressure test – a dynamic test gives the sample bond strength of 4.4 ± 1.0 MPa. It is the average strength for the 7 samples tested. Fig. 11 shows the He leak rate plots of the tested two samples. The detection limit of fine leaks of the samples for observation times of 20 minutes is between 1.0×10^{-7} std. cc/s to 4.7×10^{-9} std. cc/s.

4.1 Chemical analysis

XPS results provide important information about the structure of the interfaces that formed as result of the laser irradiation and heating during the joint fabrication process. The spectra were collected on the broken lap shear tested samples where there is exposed bond line on the failed surfaces that means the failure was in Imidex. The XPS C 1s line high-resolution (multiplex, Shirley baseline subtracted) spectrum is shown in Fig. 12 as a function of the depth of sputtering (i.e., sputtering time). At the surface (0 s sputtering, bottom), the spectrum corresponds to one from a Imidex surface with contributions from carbonyl groups (close to 288eV) and other types of C environments that form the Imidex polymeric molecular structure [19]. Upon sputtering the carbonyl group line disappears, the intensity (both total and relative to each other) of the other contribution changes, and, most significantly, a new line at around 281eV, associated with Ti-C bonds, appears and becomes stronger (see especially the spectrum at 1200 s of sputtering). The Ti 2p spectra are shown in Fig. 13. The spectra taken from the surface correspond to fully oxidized Ti, i.e. TiO_2. Deeper in the substrate, after 1200 s of sputtering the spectra consist almost entirely of pure metallic Ti: the 2p doublet is shifted downward by about 6 eV. Between these two extreme cases, we observe a mixture of states that evolve from pure oxide to pure metal with the increase of the sputtering time. These intermediate chemical states can be interpreted in terms of a mixture of oxidized states. Some of these states could be associated with Ti-C bonds as revealed by the C1s spectra. The O1s XPS spectra (not shown) taken from the surface show several peaks, some of which come from the adsorbed oxygen at the surface and some from the TiO_2 and the PI. Upon sputtering, the adsorbed oxygen line disappears and only oxygen engaged in various Ti oxides is observed in agreement with what was described above for the C1s and Ti 2p XPS line cases.

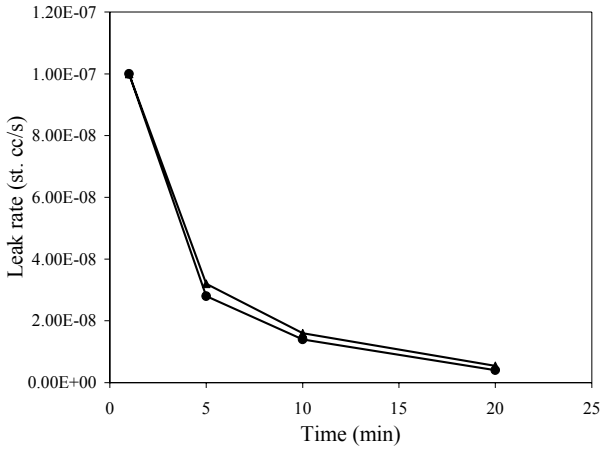

Fig. 11 He leak pattern of a fiber laser joined Ti coated glass/PI sample.

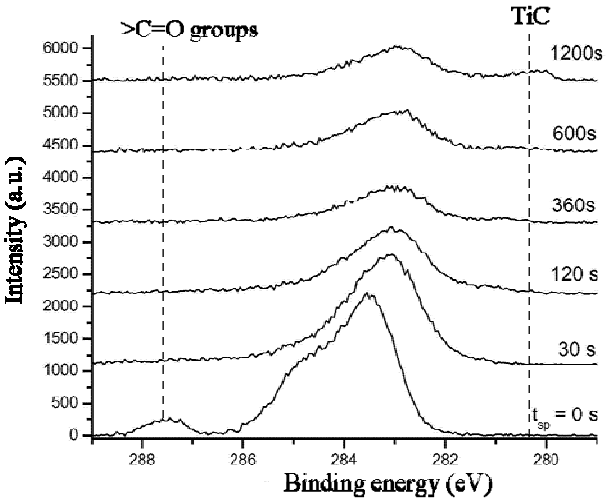

Fig. 12 XPS C 1s spectra from the Ti coated glass side as a function of Ar ion sputter time.

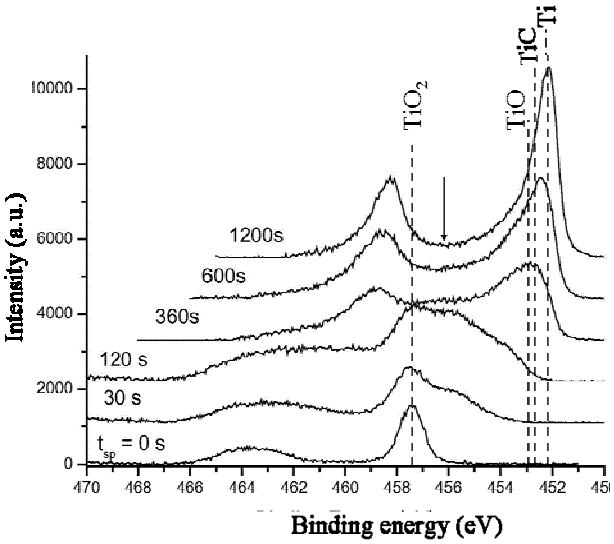

Fig. 13 XPS Ti 2p spectra from the Ti coated glass side as a function of Ar ion sputter time. The spectrum at the interface (30s sputtering) has one new component at binding energy of 456 eV shown by the downward arrow.

4.1 Failure mode analysis

After testing the bond strength of the samples – the failed bond surfaces were analyzed under optical microscope. Fig. 14 and 15 show the common failure pattern of the lap shear tested and pressure tested samples respectively. Along the joint line broken glass pieces are observed. During Ti coating some residual stress should have introduced in glass and also during laser joining thermal residual stress have developed in the bond due to mismatch of coefficient of thermal expansion (CTE) between Ti coating, glass and Imidex. During transient heating Ti having greater CTE will impose a tensile stress over glass that is weak in tensile load. If the transient residual stress exceeds glass tensile strength, glass will crack. The weakening of the glass near the surface is proven from micro Raman analysis in our earlier work [20]. The exposed bond lines (Fig. 14 & 15) of lap shear and pressure test specimens were analyzed by SEM. Mixed mode failure (Fig. 14) - both bond and glass failure is prominent for lap shear specimens. However, for the pressure test specimen (Fig. 15), there is clean glass failure that predominate the failure process.

SEM pictures reveal that in the exposed area of the failed joints has Imidex residue on it. But the amount of Imidex sticking on the joint and the failure mechanism of the plastic is quiet different in both cases. The lap shear samples have a large quantity of Imidex residue indicating quite strong bond (Fig. 16). Whereas, the pressure tested miniature samples have little Imidex on the bond line and the mode of failure is also different (primarily glass failure) indicating much weaker strength as found from the result (Fig. 17). Also, it is noted that the ductile surface topography of polymer exhibited in Fig. 16 is absent in Fig. 17 – the dynamic test specimen. Imidex surface shows the total heat affected zone (HAZ) due to the partial melting of plastic (Fig. 18 & 19). This is due to the Gaussian laser fluence which has highest temperatures near the peak of the profile.

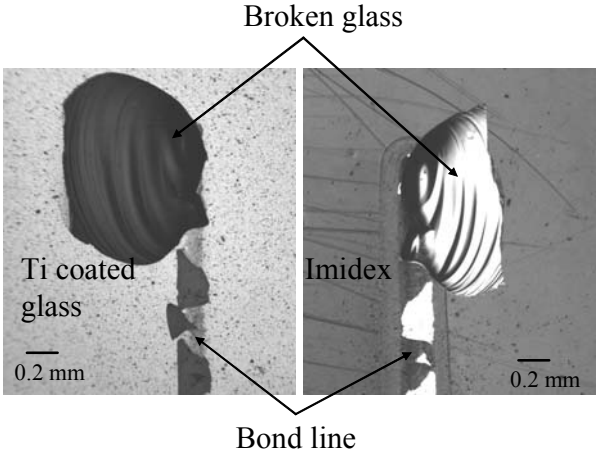

Fig. 14 Optical microscopy pictures of lap shear tested sample showing general failure pattern of the Ti coated glass/Imidex transmission laser joint. The failed bond line on both the Ti coated glass (left) and Imidex (right) surfaces has broken glass pieces and in some region exposed bond area.

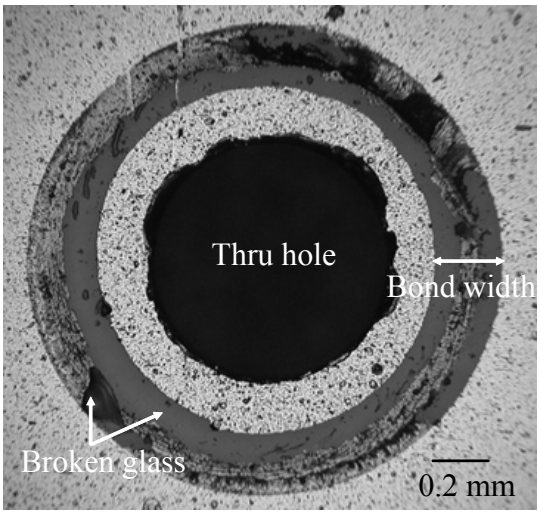

Fig. 15 Optical microscopy picture of pressure tested bond failure pattern (Ti-coated glass surface)

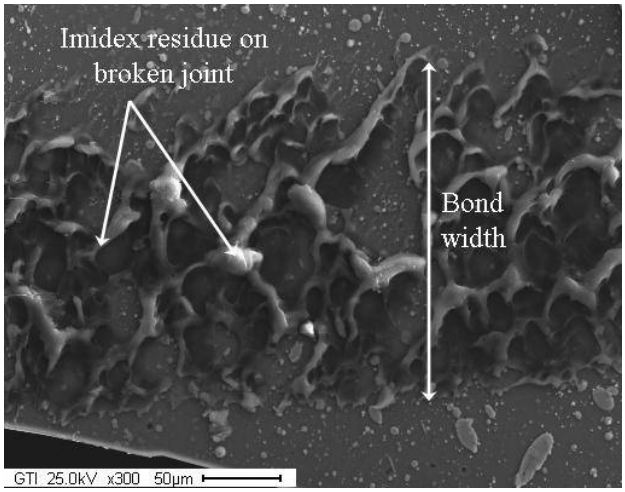

Fig. 16 SEM picture of bond area on Ti coated glass surface of lap shear tested sample showing Imidex residue on the bond line.

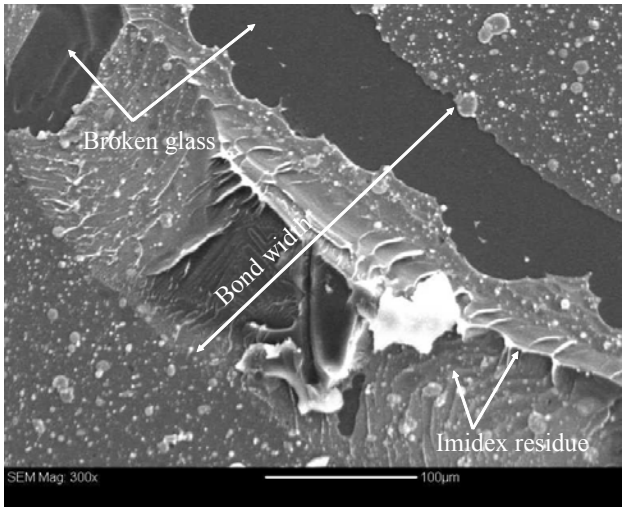

Fig. 17 SEM picture of bond area on Ti coated glass surface of pressure tested sample showing few Imidex residue on the bond line and initiation of the bond failure in glass near the hole through which high pressure is applied.

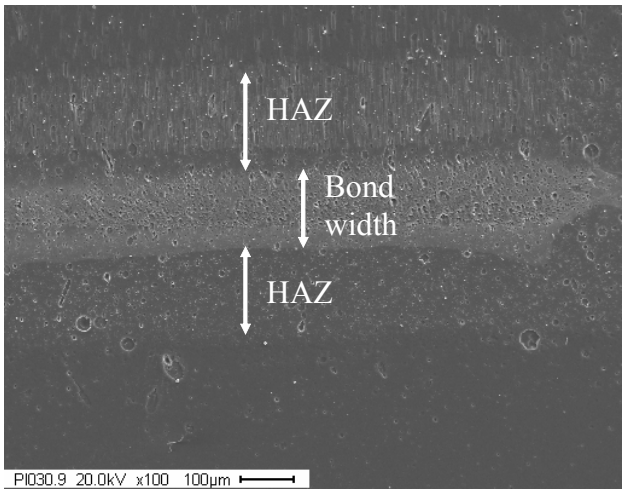

Fig. 18 SEM picture of bond area on Imidex surface of lap shear tested sample showing HAZ near the bond line.

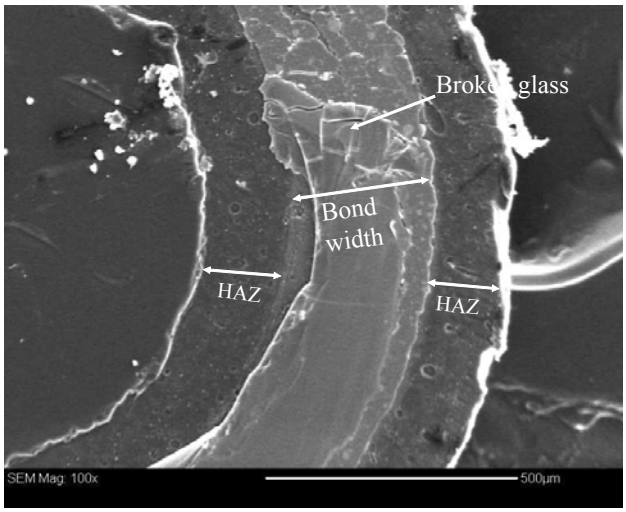

Fig. 19 SEM picture of bond area on Imidex surface of pressure tested sample showing HAZ near the bond line and broken glass layer on the bond line.

4.3 Stress analysis

Finite Element Analysis of the lap shear system showed slight bending of sample under lap shear test. Flexural stress arises because of two joined material components are not coplanar. Some of the samples may fail in flexural stress rather than lap shear stress. It is mentioned in the modeling procedure that the model was developed considering strong interfaces between titanium and polyimide, and between titanium and glass. In addition, the failure of glass substrate under tension clearly proves that the bonding between the mating substrates is truly high. Thus, the load displacement response from the FEA that is modeled considering strong interface between bi-materials has been compared with the experimental results for the samples. From Fig. 20, it is apparent that the FEA prediction matches reasonably well with the experimental data. However, the FEA results seem to over predict as compared with the experimental data. The over-estimation by FEA results could be associated with the under-estimation of the material property used and the inhomogeneity of the real interface.

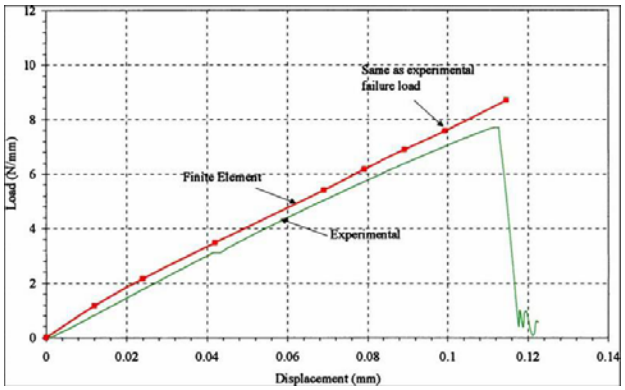

Fig. 20 Load-displacement response of the glass/polyimide sample obtained from the finite element analysis (FEA).

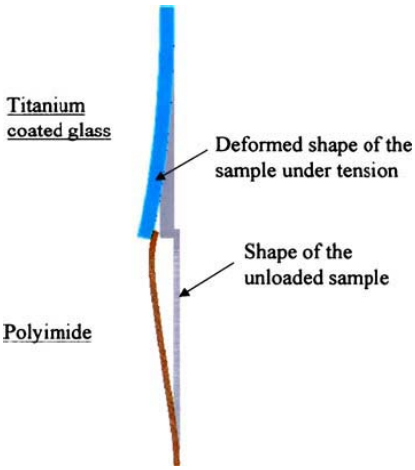

Fig. 21 Deformed shape of the Ti coated glass/Imidex sample under tension (FEA result)

The FEA prediction of the failure load of 7.3 N/mm attains at 0.1 mm displacement load as opposed to the 0.12 mm displacement as seen from the experimental data. Thus, the contour plots of various stress components discussed in the following paragraphs will be taken at the end of 0.1 mm of applied displacement load. The deformed shape of the sample under tensile load is depicted in Figure 21. It is apparent from the figure that the substrates have rotated substantially although the system was loaded with tension in y-direction. This phenomenon is common in bi-material joining systems due to the high differential deformations near the joint, and the amount of rotation depends on thickness and mechanical properties of the substrate materials. This rotation results in the development of all possible stress components with high stress gradients within the bond region. However, glass being very prone to flexural failure is expected to fail before the other substrates fail. From the contour plot of von Mises stress at 0.1 mm load, it was observed that high stress magnitudes at the two edges (Near A and B) were attained owing to the geometric singularity and material discontinuity near the edges. However, the maximum

von Mises stress was developed near the point B as shown in Figures 22.

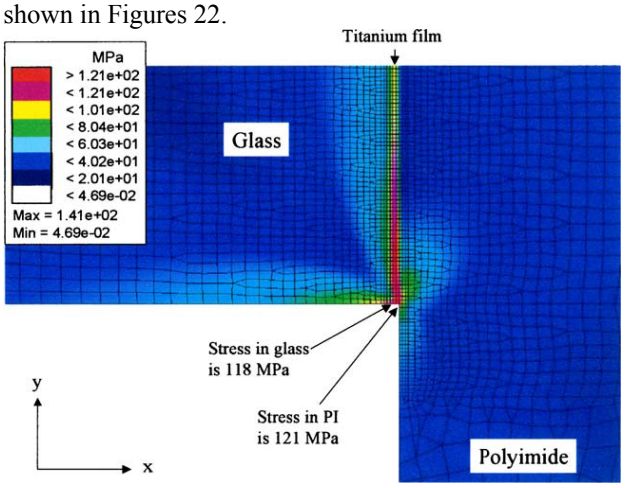

Fig. 22 Von Mises Stress distribution near location B for glass/polyimide sample under tension at 0.1 mm displacement load (FEA results).

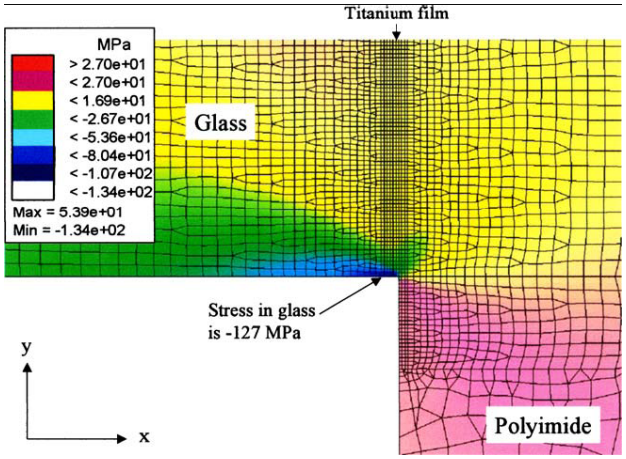

Fig. 23 x component stress distribution near the location B for glass/polyimide sample under tension at 0.1 mm displacement load (FEA results).

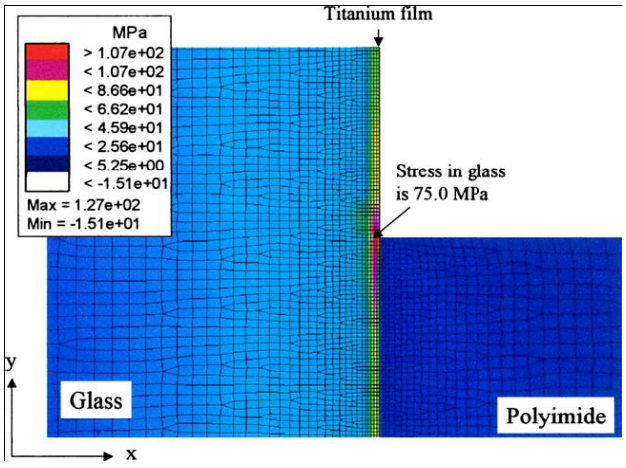

Fig. 24 y component stress distribution near the location A for glass/polyimide sample under tension at 0.1 mm displacement load (FEA results).

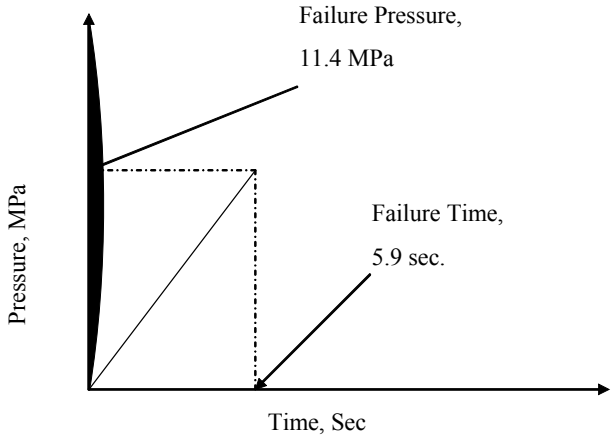

Fig. 25 Dynamic model of pressure test.

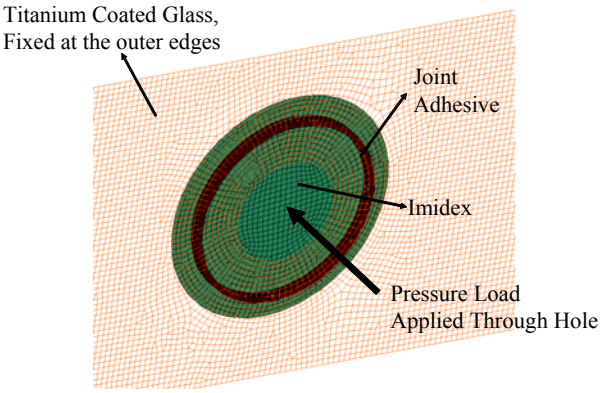

Fig. 26 Mesh view (FEA model of pressure test).

It is apparent from the figure that von Mises stresses near the point B in Imidex, Pyrex 7740, and titanium are 121.0, 118.0, 140.0 MPa, respectively. The failure strength of bulk Imidex is 118 MPa [21], and is assumed to be the same for 180 μm thin Imidex film. Thus, Imidex failure is expected to start from the location B. The stress magnitude of 118 MPa in glass is well below the compressive strength of glass (700 MPa for bulk glass). The stress in this region is compared with the compressive strength of glass as the compressive stress is developed due to joint rotation under tension. The attainment of high compressive stress is apparent from the x component stress contour, which is given in Figure 23. Now, the other singularity point A will be considered. Being a very brittle material, glass can be characterized by maximum stress failure criteria. Figure 24 shows the y component stress distribution near point A. It is observed that maximum y component stress in Pyrex glass is 75 MPa at the glass-titanium interface, which is higher than the flexural strength (69 MPa @ room temperature) of Pyrex 7740 [22]. It is mentioned here that the bending of the glass substrate in the vicinity of point A resulted in bending stress that has contributed

to additional increase in y component stress in that region. Thus the failure is expected to initiate in glass near A, and will result in partial or complete breakage of glass in the subsequent load steps. This type of failure prediction is confirmed through the microscopic images in Figure 14. The failure mechanisms observed from the experiment are shown in good agreement with the FEA predicted ones.

The dynamic model of pressure test results indicates that the failure load should be 11 MPa (Fig. 25). However our actual failure was focused to occur to average 4.4 MPa. The model is for ideal condition which does not include any potential defect and in the model no strain rate effects are considered. Observed failure modes are in the glass which is highly flaw sensitive. The model does not include this consideration. The locus of failure in the FEA model (Fig. 26) is the bonded zone. We are addressing these issues for further efforts in the modeling area to make it more accurate which will reflect the actual failure mode.

5. Conclusion

The miniature lap shear test provides a way to measure the joint strength and an alternative pressure test specimen is developed which utilizes dynamic loading for laser transmission joints. The failure modes between these two different specimens are substantially different; mixed mode vs. glass dominated for lap-shear and pressure test specimens, respectively. Interpretations of these results are provided in terms of stress analysis and related failure modes. The miniaturized hermetic specimen is found to be effective to evaluate hermeticity. The He leak rate of this system is 1×10^{-7} st. cc/s compared to the He leak rate of fully hermetic packaging system (with similar internal volume but slightly different test conditions) $<5 \times 10^{-8}$ st. cc/s [23] making the current Ti-coated glass/polyimide system near-hermetic.

Acknowledgement

Our gratitude to Dr. D. G. Georgiev for providing hermeticity test data. This work was supported by Michigan Economic Development Corp. (MEDC). Mr. Michael Psarouthakis, Program Monitor (Grant # 06-1-P1-0219)

References

1. J. Voldman, M. L. Gray, M. A. Schmidt: Annual review of biomedical engineering, 1999. **1**: p. 401-425.
2. H. Becker, L. E. Locascio: *Polymer microfluidic devices.* Talanta, 2002. **56**(2): p. 267-287.
3. G. Reed (2004) *Near-Hermetic, Thermoplastic MEMS Packages Advance.* Semicondutor International http://www.reed-electronics.com/semiconductor/article/CA420772
4. K. Gilleo (2001) *Getters — Molecular scavengers for packaging.* **Volume**, 26-29 DOI: www.hdi-online.com
5. Yu-Chuan Su, Liwei Lin: *Localized Bonding Processes for Assembly and Packaging of Polymeric MEMS.* IEEE TRANSACTIONS ON ADVANCED PACKAGING, 2005. **28**(4): p. 635-642.
6. I. Bauer, U. A. Russek, H. Herfurth, R. Witte, S. Heinemann, G. Newaz, A. Mian, D. G. Georgiev, G. Auner: *Laser microjoining of dissimilar and biocompatible materials.* Proceedings of SPIE-The International Society for Optical Engineering 2004. **5339**(Photon Processing in Microelectronics and Photonics III): p. 454-464.
7. G. Newaz, D. G.Georgiev, A. Mian, G. Auner, H. Herfurth, R. Witte: *Laser fabrication and characterization of adhesive-free joints for encapsulation of biomedical implant devices.* Materials Research Society Symposium Proceedings, 2005. **845**(Nanoscale Materials Science in Biology and Medicine): p. 267-272.
8. G. Newaz, A. Mian, T. Sultana, T. Mahmood, D. G. Georgiev, G. Auner, R. Witte, H. Herfurth: *A comparison between glass/polyimide and titanium/polyimide microjoint performances in cerebrospinal fluid.* . Journal of Biomedical Materials Research, Part A, 2006. **79A**(1): p. 159-165.
9. A. Mian, T. Sultana, G. Auner, G. Newaz: *Bonding mechanisms of laser-fabricated titanium/polyimide and titanium coated glass/polyimide microjoints.* Surface and Interface Analysis, 2007. 39(6): p506-511.
10. A. Mian, G. Newaz, L. Vendra, N. Rahman, D. G. Georgiev, G. Auner, R. Witte, H. Herfurth: *Laser bonded microjoints between titanium and polyimide for applications in medical implants.* Journal of Materials Science: Materials in Medicine, 2005. **16**(3): p. 229-237.
11. Daniel G. Georgiev, Ronald J. Baird, Golam Newaz, Gregory Auner, Reiner Witte, Hans Herfurth: *An XPS study of laser-fabricated polyimide/titanium interfaces.* Applied Surface Science 2004. **236**(1-4): p. 71-76.
12. T. Mahmood, A. Mian, M. R. Amin, G. Auner, R. Witte, H. Herfurth, G. Newaz: *Finite element modeling of transmission laser microjoining process.* Journal of Materials Processing Technology, 2007. **186**(1-3): p. 37-44.
13. *http://en.wikipedia.org/wiki/Thermal_shock*. [cited 2007 April 09].
14. *www.titanium.com/titanium/orthopedic.cfm*. [cited 2007 April 09].
15. ABAQUS User's Manual, V., Hibbit, Karlsson and Sorensen, USA.
16. T. Kuroki, A. Shibuya, M. Toriida, S. Tamai: *Melt-processable thermosetting polyimides: systhesis, characterization, fusibility and property.* Journal of Polymer Science: part A: Polymer Chemistry, 2004. **42**: p. 2395-2404.

17. M. Lu, Z. Qian, W. Ren, S. Liu, D. Shangguan: *Investigation of electronic packaging materials by using a 6 axis mini thermomechanical tester.* International Journal of Solids and Structures 1999. **36**: p. 65-78.
18. A. Mian, G. Newaz, D. G. Georgiev, N. Rahman, L. Vendra, G. Auner, R. Witte, H. Herfurth: *Performance of laser bonded glass/polyimide microjoints in cerebrospinal fluid.* Journal of Materials Science: Materials in Medicine, 2007. **18**(3): p. 417-427.
19. C. Girardeaux, E. Druet, P. Demoncy, M. Delamar, G. Chambaud: *The polyimide (PMDA/ODA) titanium interface: an experimental and theoretical study.* AIP Conference Proceedings 1996. **354** (Organic coatings): p. 46-55.
20. Daniel G. Georgiev, Taslema Sultana, Ahsan Mian, Greg Auner, Hans Herfurth, Reiner Witte, Golam Newaz: *Laser fabrication and characterization of sub-millimeter joints between polyimide ans Ti-coated borosilicate glass.* Journal of Materials Science, 2005. **40**(21): p. 5641-5647.
21. www.aurumtpi.com/aurumImidex.htm. [cited 2007 April 09].
22. www.valleydesign.com/pyrex.htm. [cited 2007 April 09].
23. MIL-STD-883E, *Test Method Standard Microcircuits.* Department of Defense, USA, 1996.

(Received: April 10, 2008, Accepted: September 3, 2008)